J Therm Anal Calorim (2010) 99:165–172
DOI 10.1007/s10973-009-0458-9

Negative thermal expansion materials

Thermal properties and implications for composite materials

Michael B. Jakubinek · Catherine A. Whitman · Mary Anne White

Japan Symposium 2008

Abstract Finite element analysis is used to explore composites of negative thermal expansion materials with positive thermal expansion materials (ZrW_2O_8 in Cu and ZrO_2 in ZrW_2O_8) and evaluate how thermal and mechanical properties, rates of cooling/heating, and geometry and packing fraction influence the overall expansion and thermal stress. During rapid temperature changes, the transient short-time thermal expansion can be considerably larger than the steady-state value. Furthermore, thermal stress in the composite can be large, especially at the interface between the materials, and can exceed the material strength.

Keywords Composites · Finite element method · Negative thermal expansion · Thermal expansion

Introduction

Many material properties change with temperature, and dimensions are among the temperature-dependent properties. The volumetric coefficient of thermal expansion, defined as $\alpha_V = V^{-1}\,(\partial V/\partial T)p$, is an intrinsic property that depends on both the material and the temperature. As thermal expansion can be anisotropic, it is also useful to consider the linear thermal expansion coefficient, $\alpha = l^{-1}\,(\partial l/\partial T)p$, where l is the linear dimension.

Thermal expansion is related to the anharmonicity of the interatomic forces: a perfect harmonic solid has $\alpha = 0$. In general, interatomic distances increase with increasing temperature, and $\alpha > 0$. At low temperatures, all materials become more harmonic, and $\alpha \to 0$ as $T \to 0$ K. Typical thermal expansion coefficients near room temperature are of the order 10^{-5} K^{-1}, with stiffer materials exhibiting lower values of α [1]. Although the thermal expansion coefficient is usually positive, in some materials it is negative in certain directions, and a few materials exhibit negative thermal expansion (NTE) in all directions, $\alpha_V < 0$ [2]. Some typical thermal expansion coefficients are shown in Fig. 1.

Zirconium tungstate, ZrW_2O_8, is a particularly interesting case because it is cubic and shows negative thermal expansion from 0.3 to 1,050 K, with $\alpha = -9 \times 10^{-6}$ K^{-1} from 2 to 350 K [3]. The negative thermal expansion in ZrW_2O_8 is related to its structure (Fig. 2): relatively rigid polyhedra are thermally excited, as the temperature increases, and rotate to pull the structure closer together as shown schematically in Fig. 3. The NTE is associated with these so-called Rigid Unit Modes (RUMs) [4]. Other materials in the same family also exhibit negative thermal expansion [5].

There is considerable interest in the possibility of combining NTE materials with normal (positive) thermal expansion materials, to reduce the potential of failure of a material or component due to thermal stress fracture. For example, NTE materials have been combined with cement [6] and epoxy [7].

M. B. Jakubinek · M. A. White (✉)
Department of Physics and Atmospheric Science, Dalhousie University, Halifax, Nova Scotia B3H 3J5, Canada
e-mail: mary.anne.white@dal.ca

C. A. Whitman · M. A. White
Department of Chemistry, Dalhousie University, Halifax, Nova Scotia B3H 4J3, Canada

M. B. Jakubinek · C. A. Whitman · M. A. White
Institute for Research in Materials, Dalhousie University, Halifax, Nova Scotia B3H 1W5, Canada

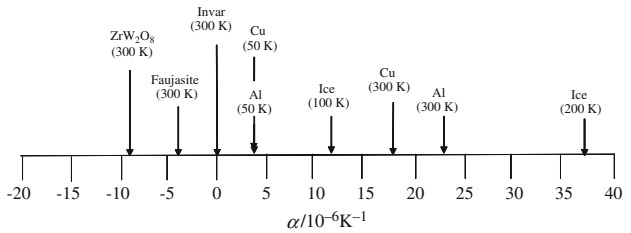

Fig. 1 Typical values of thermal expansion coefficients. Note the dependence on composition and temperature

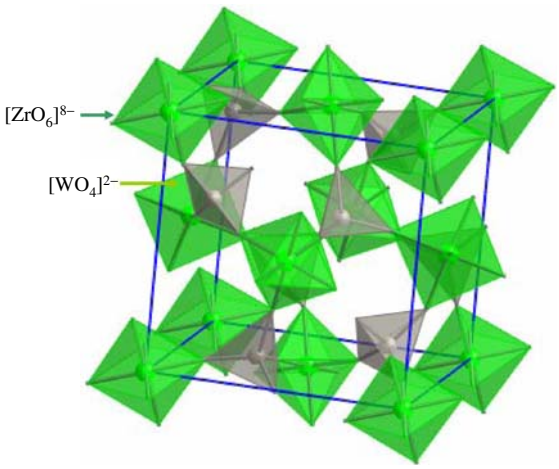

Fig. 2 Structure of ZrW_2O_8

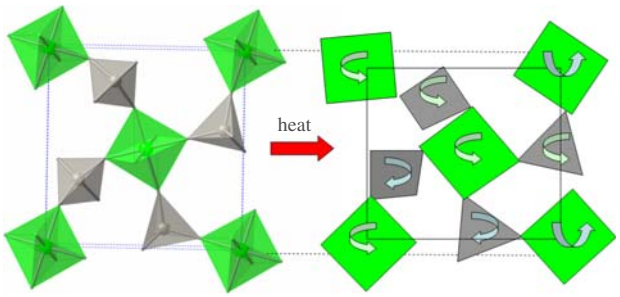

Fig. 3 Schematic view of negative thermal expansion in ZrW_2O_8 due to thermal excitation of rigid unit modes

In this article, we discuss how negative thermal expansion influences other thermal properties, namely heat capacity, thermal conductivity, the Grüneisen parameter, and thermal stress. For the design of highly thermal shock fracture resistance materials, we consider combining positive and negative thermal expansion material to achieve low thermal expansion composites. To this end, finite element analysis is used to explore different materials for low α composites and evaluate how parameters such as thermal and mechanical properties, rates of cooling/heating, and geometry and packing fraction influence the overall expansion and thermal stress in such composites.

Anomalous heat capacity

The heat capacities of many solid materials can be accurately predicted as a function of temperature from the heat capacities of the constituents; for example, the heat capacity of sodalite ($Na_8Al_6Si_6O_{24}Cl_2$) can be represented to within a few percent by that of $\{3Na_2O + 3Al_2O_3 + 6SiO_2 + 2NaCl\}$ [8]. However, the heat capacity of ZrW_2O_8 is significantly underestimated by that of $\{ZrO_2 + 2WO_3\}$, by about 50% at $T = 50$ K [9]. The main reason for the discrepancy is the additional low-frequency modes due to RUMs in ZrW_2O_8, not present in ZrO_2 or WO_3. A plot of C_pT^{-3} as a function of temperature reveals the contribution of the lowest-frequency modes as a general feature of AM_2O_8 NTE materials: see Fig. 4 for α-ZrW_2O_8 [10], cubic-$HfMo_2O_8$[11], cubic-HfW_2O_8 [12], and cubic-$ZrMo_2O_8$[9]. The most important modes both for NTE and for the anomalous heat capacity are those with frequencies < 10 meV. Whether anomalous heat capacity is *predictive* of NTE remains to be thoroughly explored.

Thermal conductivity

From the Debye model, the thermal conductivity of a simple insulating solid is given by [1]:

$$\kappa = \frac{Cv\lambda}{3}, \tag{1}$$

where κ is the thermal conductivity, C is the heat capacity per unit volume, v is the mean phonon speed and λ is the phonon mean free path. In most insulating solids, optic phonons do not influence the overall thermal conductivity. However, because ZrW_2O_8 has a relatively large number of atoms per unit cell (44), one could expect the low-

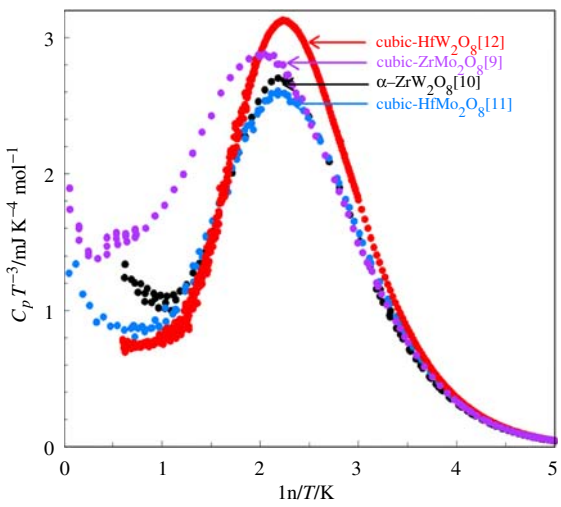

Fig. 4 Anomalous heat capacity in AM_2O_8 materials

frequency optic phonons of NTE materials to be in the correct frequency range to interfere with the heat-carrying acoustic phonons [13]. Indeed, this has proven to be the case, and the thermal conductivities of ZrW_2O_8 and $HfMo_2O_8$ are both very low and close to the theoretical minimum thermal conductivities for their lattices [10, 14].

Grüneisen parameter as a measure of anharmonicity

The Grüneisen parameter, γ, is a direct measure of the anharmonicity of a material. It can be determined per mode i as $\gamma_i = -(\partial \ln v_i/\partial V)T$ where v_i is the frequency of mode i, and deviations of γ_i from zero are quantitative indications of anharmonic interactions. Often the required information to understand each mode is not available, but the overall Grüneisen parameter, γ, can be determined from bulk thermodynamic properties:

$$\gamma = \frac{3BV\alpha}{C_V}, \tag{2}$$

where B is the bulk modulus. We have determined γ for ZrW_2O_8 and $HfMo_2O_8$ and have found large deviations from zero at low temperature (and $\gamma < 0$ due to NTE), indicative of highly anharmonic interactions [10, 14]. The magnitudes of γ scale with the NTE, i.e., larger for ZrW_2O_8 than $HfMo_2O_8$, as one might expect since both $\gamma \neq 0$ and $\alpha \neq 0$ are indications of anharmonicity. Furthermore, highly anharmonic interactions are expected on the basis of low thermal conductivity since a perfect harmonic crystal would have infinite thermal conductivity.

Thermal shock resistance

One area of particular interest for negative thermal expansion materials is in the potential for high thermal shock fracture resistance, R_s. The thermal shock fracture resistance depends on the thermal conductivity and magnitude of the coefficient of thermal expansion as follows:

$$R_s = \frac{\kappa\sigma}{|\alpha|E}, \tag{3}$$

where E is the elastic modulus, and σ is the material strength. Materials with high R_s, such as Pyrex, can undergo large excursions in temperature while resisting fracture due to internal stresses from thermal expansion. As is the case for Pyrex, if the magnitude of the thermal expansion coefficient is very small, the thermal shock fracture resistance will be high. Therefore, making composites by combining positive and negative thermal expansion materials to achieve an overall zero thermal expansion might be useful in designing new highly thermal shock fracture resistance materials.

Thermal expansion and thermal stresses in composites

The rule of mixtures estimates a composite's material properties from the volume-weighted sum of the properties of the matrix and the dispersed phase. However, the ideal rule of mixtures for thermal expansion, giving α_{avg}, assumes that there are no voids or thermal stresses and that the elastic properties are uniform throughout the composite. Figure 5 shows the estimated thermal expansion of a composite as a function of concentration of NTE material (c_{NTE}, defined as the volume fraction of NTE material) from the rule of mixtures along with an analytical model from Klemens for thermal conductivity of composite composed of spheres in a matrix [15]. The Klemens model is based on the strain field of inclusions of mismatched volume. Interestingly, it shows quite different results for ZrW_2O_8 in copper compared with copper in ZrW_2O_8, whereas the rule of mixtures would have the same α_{avg} for both. Samples of 45–65 vol% ZrW_2O_8 in copper were recently prepared and characterized [16]. Their measured thermal expansion coefficients were greater than predicted by the rule of mixtures, but less than predicted by the Klemens model.

Finite element method (FEM) modeling

The Finite Element Method is a numerical tool for solving differential equations. Numerical methods are required for

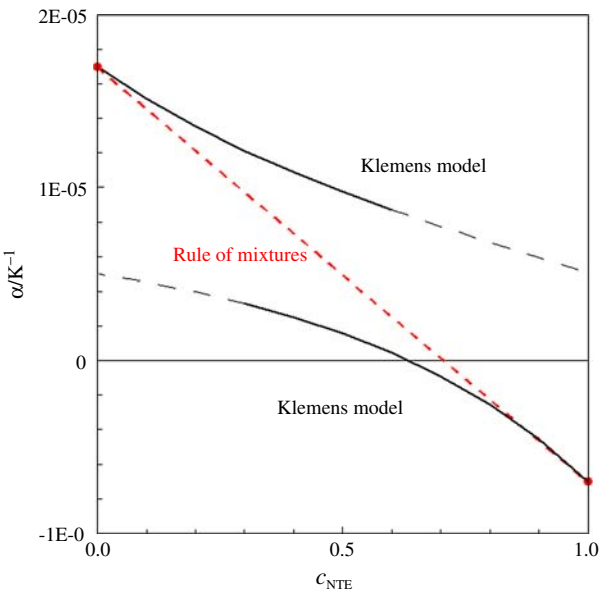

Fig. 5 Thermal expansion of ZrW_2O_8 spheres in Cu and vice versa from rule of mixtures model compared to Klemens model [15]

understanding realistic situations such as complicated geometries and boundary or time conditions, where no analytical solutions are possible. FEM divides the geometry of the material into small pieces (elements) that are joined at points (nodes), and algebraic equations can be used to describe the system at the nodes. FEM simulations were performed here using a commercial package, Comsol Multiphysics v3.5. One finite element anaylsis of close-packed tetrahedra ZrW_2O_8 (60 vol%) in copper has been published previously [17]. The present study includes a wider range of compositions, more realistic morphologies, and ZrW_2O_8 in two different types of composites.

For the simulations of composite materials, it was assumed that displacements due to thermal expansion are small and thus the materials can be treated as linearly elastic. Also, because the dynamics of the structure can be considered static compared to the time scale of the heat transfer problem, solutions can be obtained by coupling a steady-state structural mechanics problem to a transient temperature response. Comsol Multiphysics then solves the thermal and structural problems simultaneously. At each timestep, the temperature field, given by:

$$\rho C_p \frac{\partial T}{\partial t} = \nabla \cdot (\kappa \nabla T), \tag{4}$$

is first solved, where ρ is density, C_p is the specific heat, and κ is thermal conductivity. The stress–strain analysis:

$$\sigma = \boldsymbol{D}(\varepsilon_{\text{thermal}}), \tag{5}$$

is then performed using the computed temperature field at each time step, where σ is the stress vector, $\varepsilon_{\text{thermal}}$ is the thermal strain vector and $\boldsymbol{D}$ is the elasticity matrix. Note that in this case the only strains are due to thermal expansion, although additional terms could be added to include initial strain or strain due to other forces. Equations 4 and 5 are solved for specified initial and boundary conditions, here chosen so that the composite starts under zero stress and at uniform temperature and is allowed to expand/contract freely. The cooling rate was varied by changing the temperature boundary condition on the outer surfaces.

The 2D simulation geometry is shown in Fig. 6. Both components were treated as isotropic and their properties at all locations were considered to be those of the bulk (i.e., no interface effects). The center cell is considered representative of the bulk and was simulated with a finer mesh. It is surrounded by additional NTE/Cu cells, on a square array, placed to account for the influence of neighboring NTE particles on the center cell. A 5 × 5 array was used (We found only minimal differences between 5 × 5 and larger arrays). For this arrangement, c_{NTE} can be determined from the ratio, x, of the NTE particle diameter to the size of the square cell,

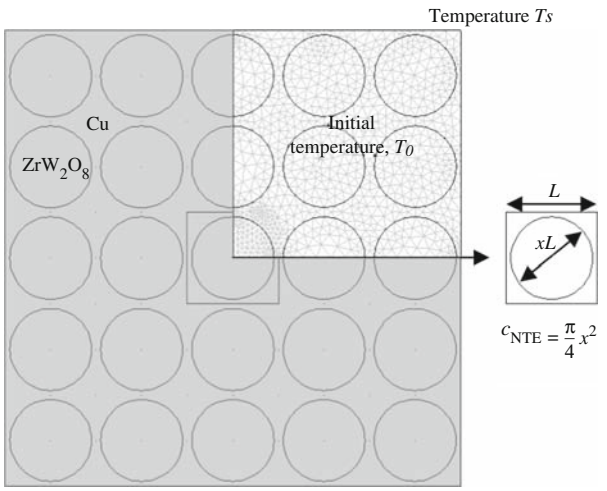

Fig. 6 Two-dimensional model of NTE in Cu composite

$$c_{\text{NTE}} = \frac{\pi}{4}x^2. \tag{6}$$

As shown in Fig. 6, the geometry is symmetric so it is necessary to simulate only ¼ of the system. Symmetry is enforced by temperature insulation and "roller" (i.e., zero displacement in the perpendicular direction) boundary conditions along the x- and y-axes. The 2D model is employed due to its simplicity in comparison to 3D models, which allows for faster solutions with finer meshes and inclusion of more neighbors. The 2D array is analogous to a 3D array of cylinders, but we found that the maximum stresses in the 2D model also are quantitatively similar to the maximum stresses in a 3D array of spheres of the same diameter (Note, however, that a 3D array of spheres has a significantly lower c_{NTE} than a 2D array of equal diameter circles and, therefore, the overall expansion coefficient would differ).

This FEM model allows for the determination of stresses and overall expansion in the system. The parameters used in the FEM simulation of the ZrW_2O_8/copper composite are given in Table 1. A composite of ZrO_2 (circles) in a ZrW_2O_8 matrix was also considered using the same geometry (*vide infra*) and the corresponding properties are listed in Table 2.

FEM results and discussion

The overall thermal expansion FEM results for ZrW_2O_8 in copper are close to the experimental results from Yan et al. [16], see Fig. 7. We found that the maximum stresses and overall expansion for a given temperature change do not depend on the size of the NTE particles, only on c_{NTE}. However, there is an influence of cooling rate on expansion. Figure 8 shows the overall thermal expansion of NTE

Table 1 Parameters used in FEM simulation for ZrW_2O_8/copper composite

	ZrW_2O_8	Cu	Units
Thermal expansion coefficient, α_l	−7	17	10^{-6} K^{-1}
Poisson ratio, v	0.3	0.34	–
Elastic modulus, E	70	110	GPa
Thermal conductivity, κ	0.7	400	W m^{-1} K^{-1}
Specific heat, C	400	350	J kg^{-1} K^{-1}
Density, ρ	4,500	8,900	kg m^{-3}

Table 2 Parameters used in FEM simulation for ZrW_2O_8/ZrO_2 composite

	ZrW_2O_8	ZrO_2	Units
Thermal expansion coefficient, α_l	−7	10	10^{-6} K^{-1}
Poisson ratio, v	0.3	0.23	–
Elastic modulus, E	70	200	GPa
Thermal conductivity, κ	0.7	2	W m^{-1} K^{-1}
Specific heat, C	400	400	J kg^{-1} K^{-1}
Density, ρ	4,500	5,700	kg m^{-3}

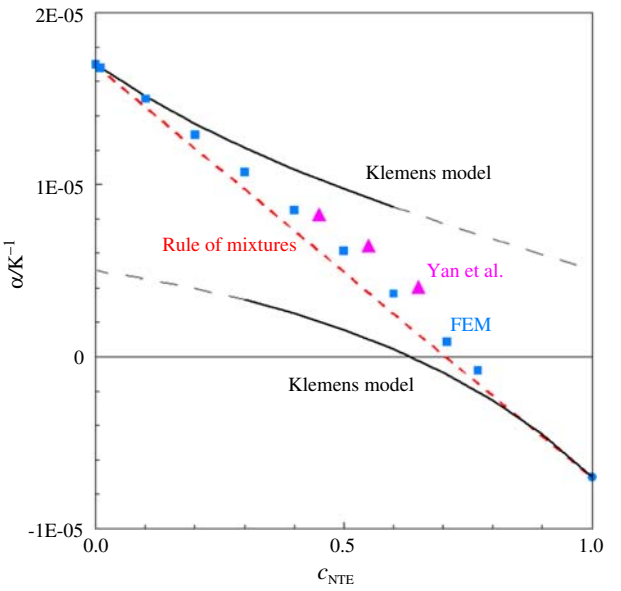

Fig. 7 Thermal expansion of ZrW_2O_8 in copper composite: FEM model shown as *squares*, Yan et al. [16] experimental results shown as *triangles*, rule of mixtures model is *dashed line*, and Klemens model is *solid line*

in copper composite as a function of time at varying cooling rates. From this figure, it can be seen that quench cooling can give larger expansion at short times because, as a consequence of the low thermal conductivity of the NTE material, copper contracts significantly before the NTE material can expand. In that case the peak and steady-state

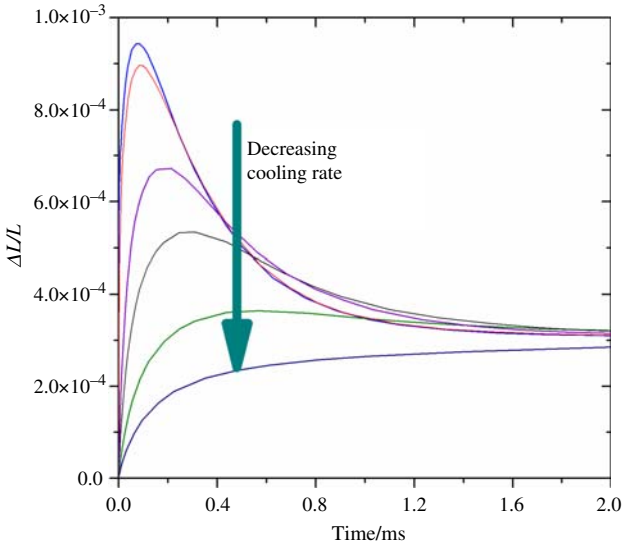

Fig. 8 Thermal expansion of NTE in copper composite as a function of time at varying cooling rates

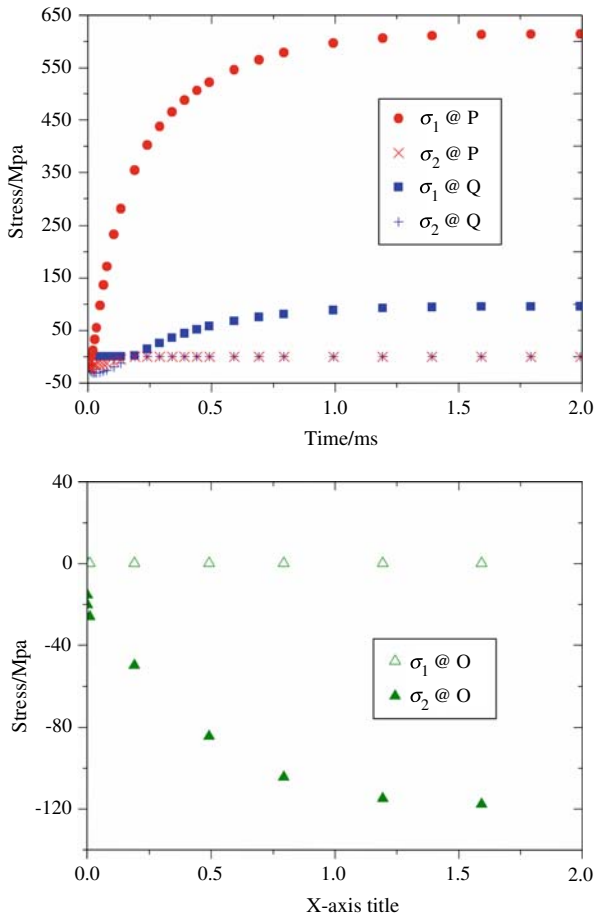

Fig. 9 Principal stresses at points O (*center of NTE particle*), P (*at NTE/Cu interface along x-axis*), and Q (*99% of the distance from O to P*) as a function of time

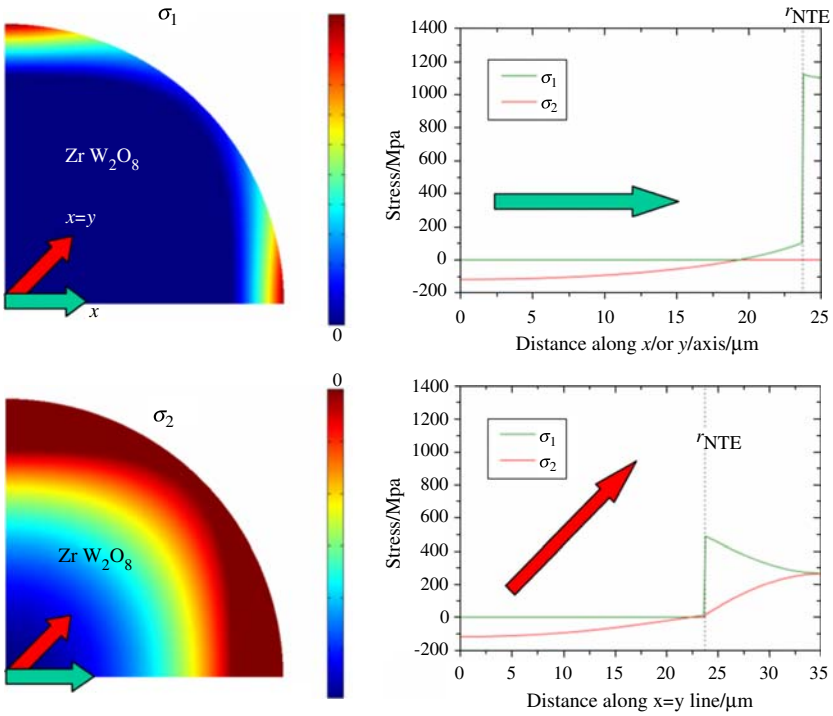

Fig. 10 Principal stress distributions in the NTE particles and principal stresses along the x axis and $x = y$ line within the center NTE/Cu cell for the composition with $\alpha_{avg} = 0$. r_{NTE} indicates the NTE/Cu interface. In colour online

expansions are still independent of particle size, but the time at which the peak occurs is size-dependent.

For the determination of thermal stresses for the ZrW_2O_8 in copper composite, we simulated a 350 K drop in temperature. The largest stresses occur at the new steady-state temperature (see Fig. 9), therefore, the maximum stresses depend on the temperature change but not the cooling rate. We also found that thermal properties (thermal conductivity and heat capacity) do not affect the maximum stresses. (These findings are in contrast to $\alpha+/\alpha+$ composites with low κ inclusions, where transient stress maxima can occur.) As a result of these factors, it is possible to focus exclusively on the steady-state stress distributions. The steady-state principal stress distributions (σ_1 and σ_2), and graphs along the $x = 0$ (or, equivalently, $y = 0$) and $x = y$ lines (see Fig. 10) show that there are large stress concentrations near the NTE/Cu interface. These stresses are a concern in terms of causing unwanted phase transitions: the maximum stress of ca. 1,000 MPa exceeds the pressure at which the $\alpha \rightarrow \gamma$ phase transition occurs in ZrW_2O_8 (ca. 300 MPa [18]), a finding supported by experimental evidence that thermally induced stress causes the phase transformation of ZrW_2O_8 in a copper matrix [16, 19]. High stresses were also found in the finite element analysis of tetrahedra of ZrW_2O_8 (60 vol%) in Cu [17]. Furthermore, the thermal stresses we observe greatly exceed the strength of ZrW_2O_8 (flexural strength ca. 15 MPa [20]).

In order to test the influence of more closely matched thermal properties of the matrix and the inclusion, the

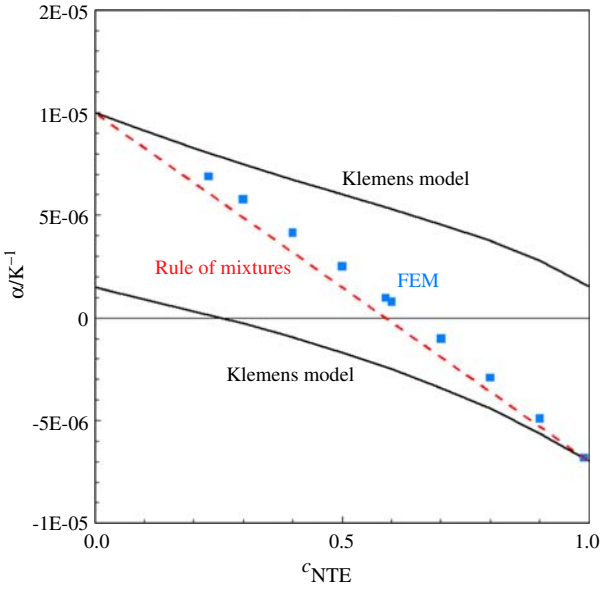

Fig. 11 Thermal expansion of ZrO_2 in ZrW_2O_8 composite from: FEM model shown as *squares*, rule of mixtures model *is dashed line*, and Klemens model is *solid line*

FEM analysis was repeated using ZrO_2/ZrW_2O_8. In this case, we used ZrW_2O_8 as the matrix (it was the inclusion in the ZrW_2O_8/Cu studies described above) because this system has been investigated experimentally [20, 21]. For ZrO_2 in ZrW_2O_8, the FEM results, shown in Fig. 11, are above the rule of mixtures, whereas, the experimental data from De Buysser et al. [20] are below the rule of

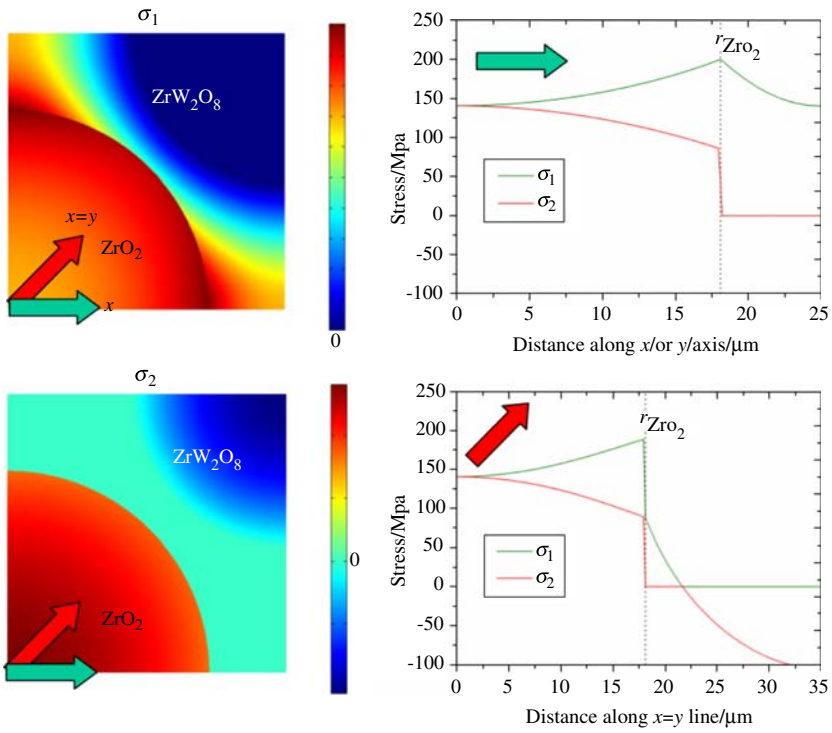

Fig. 12 Principal stress distributions and principal stresses along the x axis and $x = y$ line within the center ZrO_2/NTE cell for the composition with $\alpha_{avg} = 0$. r_{ZrO2} indicates the ZrO_2/NTE interface. In colour online

mixtures line. A likely factor in this discrepancy is the existence of voids in real samples. The elastic modulus of ZrO_2 is known to decrease with increasing porosity [22] and our simulations show that as elastic modulus is decreased, the overall expansion line moves toward, and then below, the rule of mixtures line. The difference between the actual composite morphology [20] and the simulated geometry is another factor. However, a key result of our simulations is that the steady-state stress distributions near the ZrO_2/ZrW_2O_8 interface (Fig. 12; $r = r_{ZrO2}$) are much less than in the NTE/Cu composites. In both simulations, the temperature change is -350 K and the compositions have been chosen to give $\alpha_{avg} = 0$. (Note that the amount of filler required to achieve $\alpha_{avg} = 0$ is lower for ZrO_2/ZrW_2O_8 than NTE/Cu because the magnitudes of the thermal expansion coefficients are more closely matched in the former case).

While the high thermal conductivity of copper could be desirable in a composite, the simulated stress distributions suggest that ZrO_2/ZrW_2O_8 composites might be more promising candidates than NTE/Cu composites for low expansion composites that are required to operate over a wide temperature range. However, in both the composites there is potential for transient peaks in expansion and large thermal stresses. Note that finite element studies of glass–ceramic composites show much lower stresses which can be accommodated by the viscoelastic properties of the glass matrix [23].

Conclusions

Negative thermal expansion materials in the ZrW_2O_8 family have anomalously high heat capacity at low T, large magnitudes of Grüneisen parameter, and low thermal conductivity. Composites designed to have α_{avg} close to zero can have thermal expansion coefficients that are non-zero both at short times after major temperature changes, and at steady-state conditions. However, the discrepancies between α_{avg} and observed values of α are much smaller than suggested by an analytical model [15], and the rule of mixtures provides a reasonable guide for steady-state values of the overall thermal expansion coefficient of these composites. Of more concern for mechanical stability of the system is the possibility of transient maxima in expansion at high cooling rates, and large steady-state thermal stresses in the composite. The simulations are simplified by the fact that in composites of materials with opposite signs of α, the maximum thermal stresses occur at steady-state conditions and, for given constituent materials, are determined only by the temperature change and c_{NTE}. Thermal stresses are larger when the amount of filler is larger and hence it is advantageous to use components with similar magnitudes of α. Given the thermal stresses that can develop in a composite when subjected to a large temperature change, sufficient to cause phase transitions or brittle failure, it might be more desirable to develop *pure*

materials with intrinsic, low expansion for applications in which potential for thermal stress is a major concern.

Acknowledgements We gratefully acknowledge D. Retallack for introducing us to FEM studies and a useful discussion with J. Zwanziger. This study was supported by NSERC of Canada, the Killam Trusts and the Sumner Foundation, along with the Canada Foundation for Innovation, and Atlantic Innovation Fund and other partners that fund the Facilities for Materials Characterization managed by the Institute for Research in Materials at Dalhousie University.

References

1. White MA. Properties of materials. New York: Oxford University Press; 1999.
2. Barrera GD, Bruno JAO, Barron THK, Allan NL. Negative thermal expansion. J Phys Condens Matter. 2005;17:R217−52.
3. Evans JSO, Mary TA, Sleight AW. Negative thermal expansion materials. Phys B. 1998;241:311–6.
4. Pryde AKA, Hammonds KD, Dove MT, Heine V, Gale JD, Warren MC. Origin of the negative thermal expansion in ZrW_2O_8 and ZrV_2O_7. J Phys Condens Matter. 1996;8:10973−82.
5. Sleight AW. Negative thermal expansion. Therm Conduct. 2006;28:131−9.
6. Kofteros M, Rodriguez S, Tandon V, Murr LE. A preliminary study of thermal expansion compensation in cement by ZrW_2O_8 additions. Scr Mater. 2001;45:369−74.
7. Miller W, Smith CW, Dooling P, Burgess AN, Evans KE. Tailored thermal expansivity in particulate composites for thermal stress management. Phys Status Solidi B. 2008;245:552−6.
8. Qui L, White MA. The constituent additivity method to estimate heat capacities of complex inorganic solids. J Chem Educ. 2001;78:1076−9.
9. Stevens R, Linford J, Woodfield BF, Boerio-Goates J, Lind C, Wilkinson AP, et al. Heat capacities, third-law entropies and thermodynamic functions of the negative thermal expansion materials, cubic α-ZrW_2O_8 and cubic $ZrMo_2O_8$, from T = (0 to 400) K. J Chem Thermodyn. 2003;35:919−37.
10. Kennedy CA, White MA. Unusual thermal conductivity of the negative thermal expansion material, ZrW_2O_8. Solid State Commun. 2005;134:271−6.
11. Kennedy CA, White MA, Wilkinson AP, Varga T. Heat capacity, lattice dynamics, and thermodynamic stability of the negative thermal expansion material $HfMo_2O_8$. Phys Rev B. 2007;75:224302-1−224302-9.
12. Yamamura Y, Nakajima N, Tsuji T, Iwasa Y, Saito K, Sorai M. Heat capacity and Grüneisen function of negative thermal expansion compound HfW_2O_8. Solid State Commun. 2002;121:213−7.
13. Murashov V, White MA. Thermal conductivity of insulators and glasses. In: Tritt TM, editor. Thermal conductivity: theory, properties, and applications. New York: Kluwer Academic/Plenum Publishers; 2004. p. 93–104.
14. Kennedy CA, White MA, Wilkinson AP, Varga T. Low thermal conductivity of the negative thermal expansion material, $HfMo_2O_8$. Appl Phys Lett. 2007;90:151906-1−151906-3.
15. Klemens PG. Thermal expansion of composites. Int J Thermophys. 1986;7:197−206.
16. Yan X, Cheng X, Xu G, Wang C, Sun S, Riedel R. Preparation and thermal properties of zirconium tungstate/copper composites. Mat-wiss. 2008;39:649−53.
17. Yilmaz S, Dunand DC. Finite-element analysis of thermal expansion and thermal mismatch stresses in a Cu–60vol% ZrW_2O_8 composite. Compos Sci Technol. 2004;64:1895−8.
18. Petorottoni CA, da Jornada JAH. Pressure-induced amorphization and negative thermal expansion in ZrW_2O_8. Sci. 1998;280:886−9.
19. Yilmaz S. Thermal mismatch stress development in Cu–ZrW_2O_8 composite investigated by synchrotron X-ray diffraction. Compos Sci Technol. 2002;62:1835−9.
20. De Buysser K, Lommens P, de Meyer C, Bruneel E, Hoste S, van Driessche I. ZrO_2-ZrW_2O_8 composites with tailor-made thermal expansion. Ceram-Silik. 2004;48:139−44.
21. De Buysser K. Negative thermal expansion in substituted ZrW_2O_8 and its ceramic composites. PhD Thesis. Universiteit Gent; 2007.
22. Munro RG. ZrO_2 (monoclinic). In: Elastic moduli data for polycrystalline ceramics. National Institute of Standards and Technology. 2002. http://www.ceramics.nist.gov/srd/summary/ZrO2m.htm. Accessed 31 Aug 2009.
23. Ganghoffer J-F. Calculation of thermal stresses in glass-ceramic composites. Mech Time Depend Mater. 2000;4:359−79.